Niels C. Rattenborg, Steven L. Lima, Charles J. Amlaner
Department of Life Sciences, Indiana State University, Terre Haute, Indiana 47809, USA
e-mail: lsratten@scifac.indstate.edu

1. Ball, N. J., Amlaner, C. J., Shaffery, J. P. & Opp, M. R. in *Sleep '86* (eds Koella, W. P., Obál, F., Schulz, H. & Visser, P.) 151–153 (Fischer, New York, 1988).
2. Oleksenko, A. I., Mukhametov, L. M., Polyakova, I. G., Supin, A. Y. & Kovalzon, V. M. *J. Sleep Res.* **1,** 40–44 (1992).
3. Lima, S. L. *Adv. Study Behav.* **27,** 215–290 (1998).
4. Elgar, M. A. *Biol. Rev.* **64,** 13–33 (1989).
5. Amlaner, C. J. & Ball, N. J. in *Principles and Practice of Sleep Medicine* 2nd edn (eds Kryger, M. H., Roth, T. & Dement, W. C.) 81–94 (Saunders, Philadelphia, 1994).
6. Hoffmann, R. F., Moffitt, A. R., Shearer, J. C., Sussman, P. S. & Wells, R. B. *Waking Sleeping.* **3,** 1–16 (1979).
7. Schaeffel, F., Howland, H. C. & Farkas, L. *Vision Res.* **26,** 1977–1993 (1986).
8. Bredenkötter, M. & Bischof, H.-J. *Vis. Neurosci.* **5,** 155–163 (1990).
9. Rechtschaffen, A., Gilliland, M. A., Bergmann, B. M. & Winter, J. B. *Science* **221,** 182–184 (1983).

Pattern formation in semiconductors

In semiconductors, nonlinear generation and recombination processes of free carriers and nonlinear charge transport can give rise to non-equilibrium phase transitions[1,2]. At low temperatures, the basic nonlinearity is due to the autocatalytic generation of free carriers by impact ionization of shallow impurities. The electric field accelerates free electrons, causing an abrupt increase in free carrier density at a critical electric field. In static electric fields, this nonlinearity is known to yield complex filamentary current patterns bound to electric contacts[3].

We used microwaves to apply an electric field to semiconductor samples without using electrical contacts. High-frequency electric fields ionize impurities just as d.c. fields do[4], but they do not impose inhomogeneities like electric contacts. We find that in thin n-type gallium arsenide (GaAs) epitaxial layers subjected to a uniform microwave field, circular spots of enhanced free electron density with sharp boundaries are spontaneously formed above a critical microwave threshold power. This new type of self-organized free-carrier density pattern is different from current filaments in that they are currentless; they also differ from electron-hole drops[5] as only one type of charge carrier is involved.

The spatial patterns in free electron density were made visible by photoluminescence quenching[6]. Samples cooled to low temperatures (1.8 K) were illuminated by interband light and photographed in the spectral range of the luminescence of exciton recombination and donor–acceptor transitions. With increasing microwave power P, a decrease in photoluminescence occurs at a threshold value P_+ as a result of an almost circular spot of enhanced electron density with a diameter (D_+) of about 1 mm (Fig. 1b). The diameter of the spot at the threshold is always finite and independent of the size of the semiconductor sample. This pattern formation was observed in doped samples with impurity densities of about 10^{15} per cm^3, but not in 'ultrapure' material with an impurity density of about 5×10^{12} per cm^3.

When the microwave power is increased above the threshold P_+, the diameter of the original spot increases (Fig.1b,c); at certain values of P, additional spots appear at a distance of 1 to 3 mm (Fig.1d). Decreasing the microwave power after the first spot has formed makes it smaller until it vanishes at a power of $P_- < P_+$, at a diameter $D_- < D_+$ (Fig. 1e). The pattern formation process shows a hysteretic behaviour, as it is characteristic for a first-order phase transition.

The quenching of the photoluminescence in the spots indicates that the average energy of electrons is high enough to ionize impurities and excitons in the spots. The observed structures therefore correspond to spots of high free electron density. We verified this using a sample with two parallel stripe contacts at opposite edges. When a voltage was applied across the contacts, a current filament was formed in addition to the microwave-induced spot. The current filament goes through the spot, indicating that the observed structures are regions of high free electron density.

Our findings indicate that the physical background of microwave-induced pattern formation in the electron density is the same as that of current filamentation. Both of these phenomena are based on a bistability of conductivity combined with a constraint of the external driving mechanism. In the case of current filaments, the constraint is provided by the finite current applied to the sample, whereas for microwave-induced pattern formation the external constraint must be the limited power supply from the field.

Bistability and the possibility of spatial modulation of semiconductor conductivity have been attributed to three different physical mechanisms: multilevel generation and recombination kinetics of impurities[2], runaway of electron energy due to energy-dependent electron scattering[7], and electron density-dependent screening of ionized impurity scattering[4]. For all three mechanisms, bistability vanishes below a critical density of impurities, which explains the qualitatively different behaviour of doped and ultrapure materials, for which pattern formation has not been observed.

V. V. Bel'kov*, J. Hirschinger*, V. Novák†, F.-J. Niedernostheide*, S.D. Ganichev*, W. Prettl*
**Institut für Experimentelle und Angewandte Physik, Universität Regensburg, 93040 Regensburg, Germany*
†Institute of Electrical Engineering, AV ČR, 182 02 Prague 8, Czech Republic
e-mail: wilhelm.prettl@physik.uni-regensburg.de

1. Landsberg, P. T. & Pimpale, A. *J. Phys. C* **9,** 1243–1252 (1976).
2. Schöll, E. *Nonequilibrium Phase Transitions in Semiconductors* (Springer, Berlin, 1987).
3. Ridley, B. K. *Proc. Phys. Soc.* **82,** 954–966 (1963).
4. Kozhevnikov, M. *et al. Phys. Rev. B* **52,** 4855–4863 (1995).
5. Jeffries, C. D. *Science* **189,** 955–964 (1975).
6. Eberle, W. *et al. Appl. Phys. Lett.* **68,** 3329–3331 (1996).
7. Levinson, I. B. *Sov. Phys. Solid State* **7,** 1098–1102 (1965).

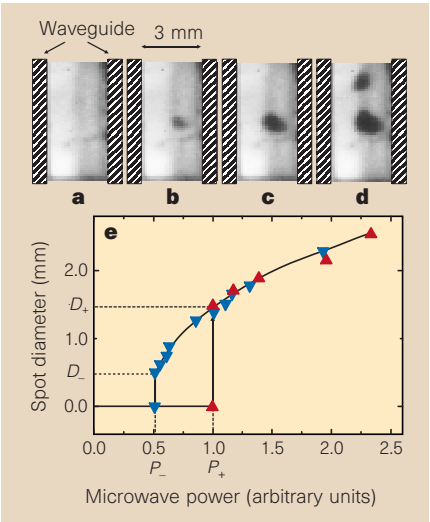

Figure 1 Self-organized formation of spots of high electron density in an n-doped gallium arsenide epitaxial layer as a result of impact ionization of shallow donors in a microwave electric field. **a–d,** Images of near-infrared luminescence for microwave power increasing from zero (**a**) to about 30 mW (**d**). Shaded stripes show the walls of a waveguide. **e,** Spot diameter as a function of microwave power. Red and blue triangles indicate increasing and decreasing power, respectively. P_+ is of the order of 10 mW.

UV-B damage amplified by transposons in maize

While absorbing visible light energy for photosynthesis, plants are unavoidably exposed to ultraviolet radiation, which is particularly harmful at shorter wavelengths (UV-B radiation). Ozone depletion in the atmosphere means that plants receive episodic or steadily increasing doses of UV-B, which damages their photosynthetic reaction centres, crosslinks cellular proteins, and induces mutagenic DNA lesions[1]. Plant adaptive mechanisms of shielding and repair are therefore critical to survival — for example, somatic tissues of maize and *Arabidopsis* defective in phenolic sunscreen pigments[2,3] incur increased DNA damage, and mutants defective in DNA repair[4,5] are killed by UV-B.

The harmful effects of UV-B on maize pollen are proportional to the exposure time[6]. I find that simulated field conditions

of UV-B exposure at 33% ozone depletion[1,6] can activate immobile *Mutator* (*Mu*) transposons[7] in maize sperm. These transposons amplify the effects of UV-B exposure by causing mutations beyond the extent of immediate DNA damage.

Mu elements, defined by shared terminal inverted repeat (TIR) ends, are regulated by *MuDR*, which encodes MURA transposase, which binds to the *Mu* TIRs[8] (Fig. 1a). When *MuDR* is transcriptionally active, *Mu* elements insert (causing mutations) and excise from existing locations (creating phenotypic variegation, a property seen as somatic spotting in pigment genes; Fig. 1b). When Mutator is inactive, *Mu* elements are methylated[7], *MuDR* transcripts are undetectable (Fig. 2), and no excision occurs (Fig. 1c). Spontaneous reactivation of somatic excision is rare (frequency $< 10^{-4}$). First-generation (F_1) inactive Mutator plants, homozygous for *bz2::Mu1* or *bz2::MuDR* reporter alleles in the anthocyanin pigment pathway, reactivate when crossed to an active Mutator *bz2* line (6 of 25 and 5 of 15 progeny ears had spotted kernels; see Supplementary Information). Reactivation crosses are more efficient with a maternal active Mutator parent (11.5% spotted kernels compared with paternal 1.9% spotted kernels). Reactivation frequency falls with each generation in which an inactive Mutator line is maintained. After three generations, reactivation occurs in fewer (3 of 29) cases and less efficiently (0.05% spotted kernels).

Irradiation of pollen with UV-B for 3 minutes restored *Mu* excision in 7 of 19 progeny ears (6.2% spotted kernels) in F_1 inactive plants. The population has considerable heterogeneity in reactivation potential as both reactivation crosses and pollen irradiation yielded progeny with a wide range of degree of spotting. Reactivation was much lower in F_3 inactive individuals, but UV-B was 14-fold more effective than crossing to a *bz2* active Mutator plant.

Maize pollen contains three haploid cells: a vegetative cell and two sperm. One sperm fertilizes the egg to form the diploid zygote, whereas the other contributes to the formation of endosperm, the tissue where somatic excision is scored. If UV-B reactivates Mutator activity in individual nuclei, usually one sperm will be reactivated (non-concordance); but if UV-B physiologically changes pollen to activate Mutator secondarily, both sperm could be affected (concordance). I therefore checked whether kernels with spotted endosperm produced a plant that transmitted reactivated Mutator to the next generation and found that UV-B induced 19 spotted:1,020 bronze kernels; none of the 19 had progeny with spotted kernels. Of 350 plants grown from bronze siblings, nine crosses to *bz2* and 14 self-pollinations produced spotted progeny, so sperm non-concordance normally occurs.

Transcriptional activation of silent *MuDR* elements could be a nucleus-specific mechanism underlying non-concordance. To test this idea, 24 bronze progeny were germinated from an ear with 23% spotted endosperms. If embryo reactivation is similar, 54% of pools from three seedlings should have at least one individual with a reactivated Mutator system: $100(1-(0.77)^3)$. Of eight pools of bronze seedlings, four contained *mudrA* transcripts (Fig. 2), indicating that seedling transcriptional reactivation parallels visible endosperm spotting.

Doubling terrestrial UV-B (>290 nm) is cytotoxic to pollen, increasing the frequency of new mutations[6] but not by enough to impair agriculture. Activation of cryptic transposable elements, however, could increase the mutation rate. Although most transposons are transcriptionally silent and immobile, they can cause many spontaneous mutations in maize and other organisms[9]. Transposons may be activated during 'genomic shock' as an adaptive mechanism[10]. Whereas damage to DNA is immediately repaired or fixed as stable mutations, transposons produce cycles of insertion and excision long after activation.

Plants with large genomes may be particularly susceptible to destabilization. Inactive retrotransposons constitute about half of the maize genome[11] and so are a reservoir of potential mutagens. Haploid pollen is a sensitive target of UV-B irradiation. Because plants lack a dedicated germ line, mutations in somatic stem cells can be represented in subsequent gametes[12]. Normally stringent selection on the vegetative cell of haploid pollen, which directs pollen maturation and growth, counterbalances the accumulation of deleterious alleles in the diploid soma. Mutations induced in individual sperm are not subjected to such rigorous selection, because genetic activity is thought to start after fertilization. As a result, transposon activation in individual sperm could greatly increase the genetic load in higher plants.

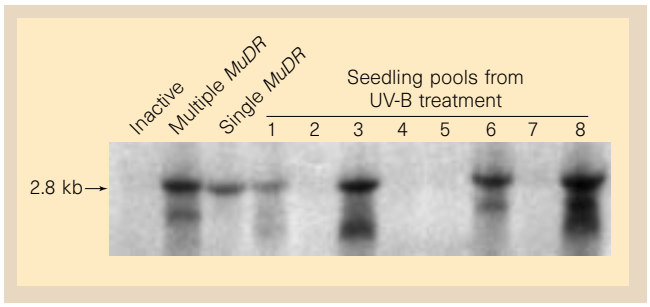

Figure 2 Northern blot to detect *mudrA* transposase transcripts. Total RNA samples were from pools of three seedlings; blots were hybridized with a *mudrA* transposase-specific probe (Fig. 1a). The 2.8-kb transcript encodes an 823-amino-acid transposase[8] required for Mutator activity; active lines produce other smaller transcripts from alternative splicing of the transposase mRNA and from internally deleted *MuDR* elements.

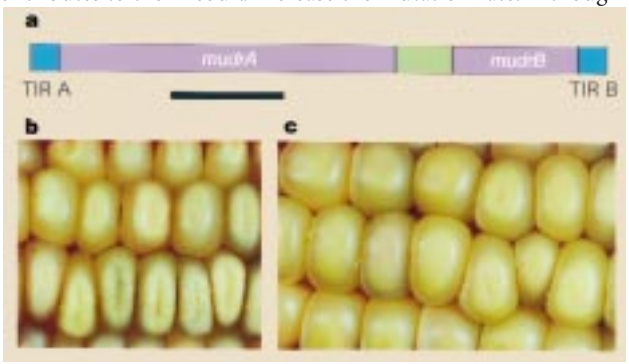

Figure 1 Mutator transposon properties. **a,** The 4.9-kilobase (kb) *MuDR* element showing the convergent transcription units of the *mudrA* transposase and helper function *mudrB* gene. Transcription initiates in the TIRs (blue) and terminates in the intergenic region (green); the *mudrA* hybridization probe region is underlined. **b,** Excision of *Mu1*, a 1.4-kb non-autonomous element sharing only the TIRs with *MuDR*, from the *bz2::Mu1* allele in a UV-B-reactivated Mutator line restores *Bronze2* gene expression in spots of anthocyanin pigmentation. **c,** No excision from *bz2::Mu1* occurs in an inactive Mutator sibling. Details of maize lines and irradiation protocols are available from the author.

Virginia Walbot
Department of Biological Sciences,
Stanford University,
Stanford, California 94305-5020, USA
e-mail: walbot@stanford.edu

1. Rozema, J., van de Staaij, J., Björn, L. O. & Caldwell, M. *Trends Ecol. Evol.* **12,** 22–28 (1997).
2. Stapleton, A. E. & Walbot, V. *Plant Physiol.* **105,** 881–889 (1994).
3. Landry, L. G., Chapple, C. C. S. & Last, R. L. *Plant Physiol.* **109,** 1159–1166 (1995).
4. Britt, A. B., Chen, J.-J., Wykoff, D. & Mitchell, D. *Science* **261,** 1571–1574 (1993).
5. Landry, L. G. *et al. Proc. Natl Acad. Sci. USA* **94,** 328–332 (1997).
6. Chrispeels, H. E. *Effects of Ultraviolet Radiation on Maize.* Thesis, Stanford Univ. (1996).
7. Walbot, V. *Mol. Gen. Genet.* **234,** 353–360 (1992).
8. Benito, M.-I. & Walbot, V. *Mol. Cell. Biol.* **17,** 5165–5175 (1997).
9. Kidwell, M. G. & Lisch, D. *Proc. Natl Acad. Sci. USA* **94,** 7704–7711 (1997).
10. McClintock, B. *Science* **226,** 792–801 (1984).
11. SanMiguel, P. *et al. Science* **273,** 765–769 (1996).
12. Walbot, V. *Trends Plant Sci.* **1,** 27–32 (1996).

Supplementary information is available on *Nature*'s World-Wide Web site (http://www.nature.com) or as paper copy from the London editorial office of *Nature*.